J Radioanal Nucl Chem (2015) 304:933–943
DOI 10.1007/s10967-014-3878-3

Sequestration of U(VI) from aqueous solutions using precipitate ion imprinted polymers endowed with oleic acid functionalized magnetite

Nikita Tawanda Tavengwa · Ewa Cukrowska · Luke Chimuka

Received: 10 November 2014 / Published online: 24 December 2014

Abstract The use of a polymeric sorbent material embedded with oleic acid coated magnetic particles as selective sorbents for the removal of U(VI) ions from industrial waste effluents was studied. In the presence of other competing ions [Th(IV) and Ni(II)], U(VI) was preferentially adsorbed. Inclusion of nano-magnetic particles in the polymer matrix aided the separation of the sorbents from aqueous solutions by application of external magnetic field. High recoveries indicated that the sorbent is suitable for application in contaminated water.

Keywords Magnetic imprinted polymer · Precipitate · Uranium · Oleic acid

Introduction

Although uranium is only present in minute concentration in seawater, its recovery from the ocean has been under serious consideration for several decades with a view for enhancing uranium reserves and avoiding the environmental impact of uranium mining [1]. Uranium is a potential environmental pollutant, especially in mining industrial wastewater, and its migration in nature is therefore important in this context. In view of the anticipated exhaustion of terrestrial uranium reserves in the near future, research has been directed towards the recovery of uranium from many sources which include natural waters [2]. Various methods have been reported regarding the removal of heavy metals from wastewaters which include thermal, biological, physical, and chemical treatments [3–5]. However, most of these methods are expensive and difficult to implement. There is therefore a serious need for the development of easy and low cost methods. Adsorbents are the most important materials examined for the removal of toxic metal ions due to their inexpensive and effective nature. Adsorption processes provide a feasible treatment, especially if the adsorbent is inexpensive and readily available [5–7].

Many organic and inorganic adsorbents containing different functional groups, which show sequestration of uranyl ions have been synthesized and used for the separation of uranium from aqueous solutions [8]. Most inorganic adsorbents have limitations on adsorption rates and have poor mechanical stability under marine conditions [9, 10]. On the other hand, numerous investigations have been carried out on organic adsorbents and have shown good uranium loadings [11, 12]. However, one of the main reasons for many traditional sorbents not becoming that much popular is their non-specific removal of a particular analyte from complex matrix.

An alternative approach involves the use of biomimetic receptor systems, or plastic antibodies capable of binding target analytes with high affinities and selectivities on par with natural receptors [13, 14]. Molecular or ion imprinting is one such technique, and is generally defined as a synthetic approach by which a molecular receptor is assembled via template-guided synthesis [15, 16]. The binding sites are created by polymerizing functional and cross-linking monomers in the presence of the target. At low pH, uranium normally exists as a uranyl ion and was used as a template in this research. Hydrolysis of the uranyl ions in aqueous solution is significant at high pH values. A larger number of uranyl hydroxides, oxyhydrates and uranates are known [17]. Studies have been done on the uptake of uranium using the imprinting technique [18–21].

N. T. Tavengwa (✉) · E. Cukrowska · L. Chimuka
School of Chemistry, Molecular Sciences Institute, University of Witwatersrand, Private Bag 3, Johannesburg 2050, South Africa
e-mail: nikita.tavengwa@students.wits.ac.za

Ion-imprinted polymers cannot be separated rapidly and effectively after treatment from polluted water. If the ion-imprinted polymers encapsulating Fe_3O_4 as magnetic cores could be synthesized, the adsorbing polymers would be separated easily by use of external magnetic fields, replacing the centrifugation and filtration processes in a convenient and economical way.

This paper discusses the preparation of magnetic uranyl(VI) IIP particles synthesized by thermal co–polymerization and consequently, the adsorption properties for uranium(VI) by U(VI) ion–imprinted polymer composite magnetic particles (IIP) and their corresponding controls, U(VI) non ion-imprinted polymer (NIP). Inclusion of the magnetic materials was to facilitate the removal U(VI) loaded sorbents and only a few studies have been reported on uranium magnetic ion imprinted polymers [22, 23]. Recently, we also reported on the uptake behaviour of uranyl ions unto bulk polymers embedded with γ-methacryloxypropyltrimethoxysilane (γ-MPS) coated magnetite [24]. The combination of magnetic nano-particles and functional monomers used in this work for the synthesis of magnetic uranium IIPs by precipitation have not been reported before.

Materials and methods

Materials

These chemicals were used to prepare magnetic polymers: $FeCl_2{\cdot}4H_2O$, $FeCl_3{\cdot}6H_2O$, NH_4OH, methanol, ethylene glycol dimethacrylate (EGDMA), methacrylic acid (MAA), 1,1′-azobis(cyclohexanecarbonitrile), salicylaldoxime (SALO), 4-vinylpyridine (4–VP), 2–methoxyethanol, $NaHCO_3$ leachant and oleic acid (OA), all purchased from Sigma Aldrich (Steinheim, Germany). The imprint source, uranyl nitrate ($UO_2(NO_3)_2{\cdot}6H_2O$) was bought from BDH Chemical Ltd (Poole, England) while $Th(NO_3)_4{\cdot}xH_2O$ and $Ni(NO_3)_2{\cdot}6H_2O$ were purchased from Sigma Aldrich (Steinheim, Germany). Analytical grade solutions from Merck (Darmstadt, Germany) were used to prepare different buffer systems: HCl/KCl was used pH for 1 and 2, Na_2HPO_4/citric acid was used for pH 3, CH_3COOH/CH_3COONa was used for pH 4, 5 and 6 and borax/H_3BO_3 was used for pH 7, 8 and 9.

Stock solutions (1,000 mg L^{-1}) of U(VI), Ni(II) and Th(IV) were prepared by dissolving an appropriate amount of dried analytical grade salt in deionized water. Working solutions were then prepared whenever needed from the stock solutions through serial dilutions, and stored at 4 °C when not in use.

ICP–OES Spectro Genesis End-on-plasma (Spectro, Germany) was used for the determination of the metals' concentration in multi-elemental solutions. AAS measurements were made on a PG-990 AAS (Leicestershire, UK) with pyrolytically coated HGA-76 graphite furnace. All pH measurements were performed on a 766 Calimatic pH meter equipped with a Shott N61 pH electrode from Knick (Berlin, Germany). In batch adsorption studies, a Laser Photo/Contact Tachometer DT-1236L from Lutron (Taipei, Taiwan) was used to measure the rotational speeds of the magnetic stirrers. A LECO-932 CHNS analyser from LECO Corporation (Michigan, USA) was used to determine the amount of carbon and hydrogen in the organic moiety which coated the magnetite. Fourier-transform infrared spectra were recorded in the frequency range of 400–4,000 cm^{-1} using a Tensor 27 Bruker FTIR spectrometer (Ettlingen, Germany). Raman spectra were acquired using a Jobin–Yvon T64000 Raman spectrograph from Wirsam Scientific (Pty) Ltd (Johannesburg, South Africa). Scanning electron microscopy (SEM), FEI Quanta 400 FEG ESM at 5 kV was used to explore morphological features of the magnetic particles. Magnetic properties of the synthesized particles were performed on a Cryogenic High field measurement system vibrating sample magnetometer (VSM) from Cryogenic Ltd (London, United Kingdom).

Synthesis of precipitate polymers

Precipitate polymers were synthesized by a method outlined by Singh and Mishra [25] but with increased porogen volume and endowed with magnetic particles. OA surfactant was used for coating the magnetite. To remove the excess solvent, the magnetic IIPs were then dried at 70 °C after which they were washed with ethanol and water mixture with increasing amount of water until only water was used to remove all unreacted pre-polymerization reagents. Three grams of the magnetic IIPs was transferred to a 250 mL volumetric flask upon which a 100 mL of 1 mol L^{-1} $NaHCO_3$ were added and stirred gently for 6 h. Thereafter, magnetic separation of the magnetic polymers was done and the solution retained for metal analysis. The residue was treated with freshly prepared $NaHCO_3$ leachant and the washing cycle repeated until there was no detectable uranium in the solution. Magnetic NIPs were prepared and treated likewise, except that the imprint ion was not included.

Uranium uptake experiments

Magnetic polymer amount (10–100 mg), agitation time (10–90 min) and initial U(VI) concentration (0.5–8 mg L^{-1}) were optimized. Optimization was achieved by varying one parameter while keeping the others constant, and all experiments were carried out in triplicates. In all cases, the mixtures were magnetically stirred at 1,500 rpm and a sample volume of 25 mL was used. The influence of adsorption parameters was evaluated by calculating the extraction efficiency (E) as shown in Eq. (1):

$$E = \frac{(C_o - C_e)}{C_o} \times 100 \quad (1)$$

where C_o (mg L^{-1}) is the initial concentration and C_e (mg L^{-1}) represents the final equilibrium concentration after adsorption. The adsorption capacity, q (mg g^{-1}), is defined as mass of substrate bound on a gram of adsorbent and Eq. (2) shows its mathematical calculation where C_o and C_e (mg L^{-1}) are as described in Eq. (1). V (L) is the volume of the sample solution and W (g) the mass of the adsorbent [26, 27].

$$q = \frac{(C_o - C_e)V}{W} \quad (2)$$

Point of zero charge (pHpzc)

For the point of zero charge (pHpzc) determination, 0.1 mol L^{-1} KNO_3 solution was prepared and its initial pH (pH_i) was adjusted between 1 and 12 by NaOH and HCl in different test tubes. The pH adjusted 12 mL of KNO_3 and 100 mg adsorbent were then interacted in test tubes. The samples were kept at 25 °C for 24 h and the final pH (pH_f) of solutions was measured by using a pH meter.

Selectivity of the magnetic polymers

For selectivity studies, a multi-elemental mixture of solution was made from 2 mg L^{-1} of U(VI), Ni(II) and Th(IV) ions. This solution was transferred to 25 mL vials where the optimized weight (50 mg) of the magnetic IIP was added. A batch adsorption experiment was then performed at 25 °C for a prescribed time of 45 min at 1,500 rpm. Separation of the polymers was then carried by application of a magnetic field. The metals remaining in solution were then quantified with ICP–OES or GFAAS. The respective magnetic NIP was used for the control experiment. The distribution coefficients, K_d (mL g^{-1}) of U(VI) and Ni(II) and Th(IV) were calculated using Eq. (3):

$$K_d = \frac{(C_o - C_e)V}{C_e W} \quad (3)$$

Equation (4) was used to calculate the selectivity coefficients (K) for the binding of uranyl ions in the presence of the other competing ions in a binary mixture:

$$K_d = \frac{K_d(UO_2^{2+})}{K_d(X)} \quad (4)$$

Another important parameter is the relative selectivity coefficient (K') which represents the enhanced effect of imprinting on selectivity and adsorption affinity for the template onto the magnetic polymer. The K' of the magnetic IIP against the magnetic NIP was calculated using Eq. (5) where K_{IIP} and K_{NIP} are the selectivity coefficients of the magnetic IIP and NIP, respectively.

$$K' = \frac{K_{IIP}}{K_{NIP}} \quad (5)$$

Results and discussion

Synthesis and characterization of magnetic polymers

A proposed reaction scheme for the synthesis of the magnetic U(VI) polymer is illustrated in Fig. 1. The polymerizable double bond on the γ-MPS meant that magnetite was chemically anchored within the polymeric matrix of the sorbent. This ensured that the polymers were magnetic and responded to applied external magnetic field. Addition of the coated magnetite was during cross-linking of the ternary complex.

Figure 2 shows the FTIR spectra of two magnetic particles and the OA surfactant. The absorption peaks at around 530 cm^{-1} for the bare magnetite (b) and its corresponding OA coated magnetite (c) indicated the presence of Fe–O. The band around 3,400 cm^{-1} was due to the hydroxyl groups around the magnetite since co-precipitation synthesis was carried out in aqueous solution. The two bands between 2,900 and 2,800 cm^{-1} are attributed to the asymmetric and the symmetric CH_2 stretch of the OA, respectively. Two bands at 1,441 and 1,540 cm^{-1} were for ν_s and ν_{as} of the carboxylate, respectively.

Near room temperature, magnetite very slowly oxidizes to maghemite and then at higher temperatures, to hematite through a process called martitization. The oxidation of magnetite (Fe_3O_4) to hematite (α-Fe_2O_3) proceeds either directly or via maghemite (γ-Fe_2O_3). These three phases of iron oxide (magnetite, hematite and maghemite) have very distinct bulk Raman spectra and this was used to determine the phase of the uncoated and OA coated iron oxide particles. Assignment of the band positions for phase identification was compiled by Slavov et al. [28] and is presented in Table 1, together with iron oxide and OA-iron oxide under study. The presence of the strong peaks around 667 cm^{-1} for the bare and coated iron oxide indicated that the phase of the iron oxide present was magnetite (Fe_3O_4) [29].

Carbon, hydrogen, nitrogen and sulphur (CHNS) analysis from values in Table 2 illustrated that the average ligand concentration on the magnetite was 3.82 mmol g^{-1} for OA-coated magnetite.

The surface characterization of magnetic IIP and NIP was carried out using scanning electron microscopy (SEM) (Fig. 3). The SEM images showed appreciable differences in the morphology of the two polymers. The magnetic NIP had smooth surfaces and uniform diameter of approximately 45 μm, and the regular structure of the non-imprinted

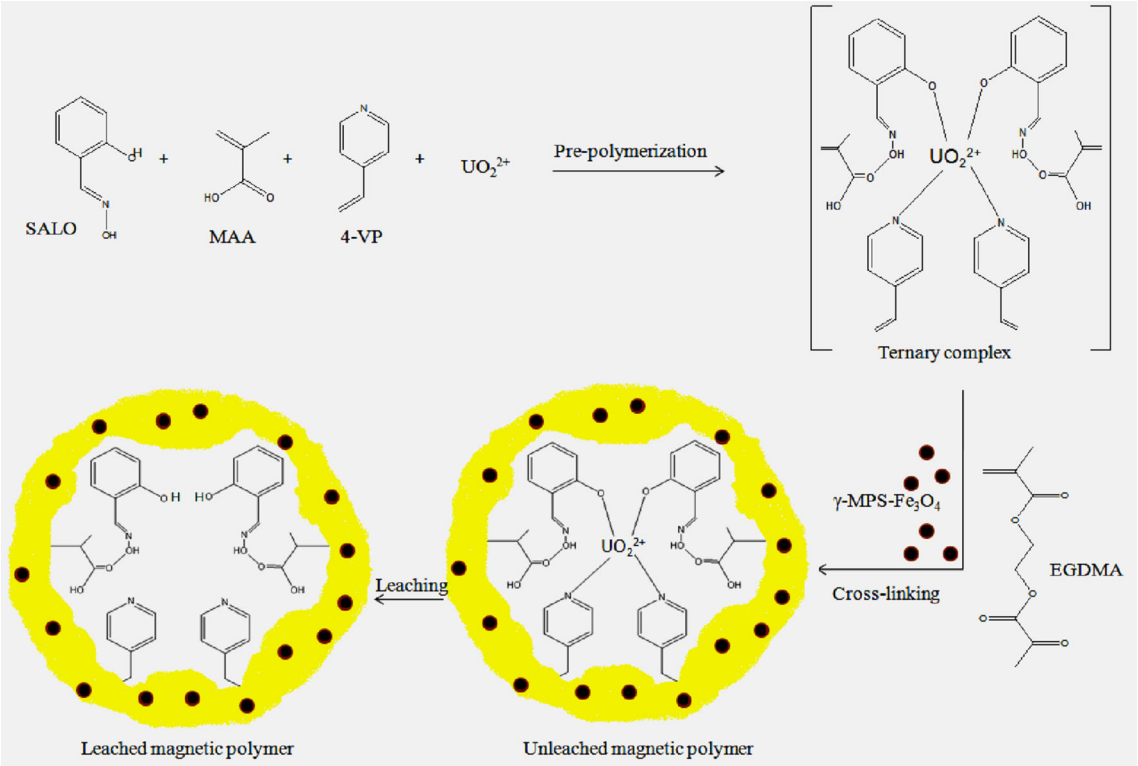

Fig. 1 Polymerization on OA functionalized Fe_3O_4 particles

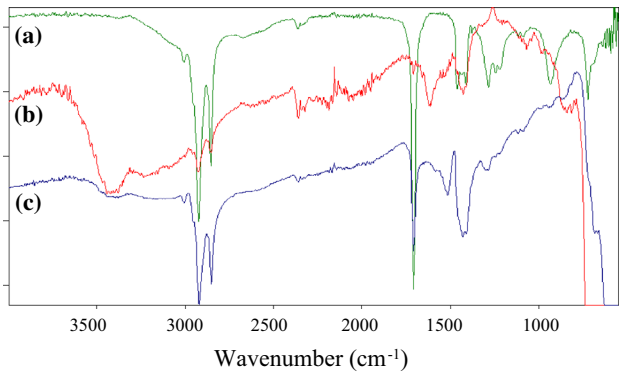

Fig. 2 FTIR spectra of **a** OA, **b** bare Fe_3O_4 and **c** OA@Fe_3O_4

Table 1 Raman bands for magnetite, maghemite and hematite

	Iron oxide	Wavelengths (cm^{-1})
Literature	Fe_3O_4 (magnetite)	193, 306, 538, 668
	γ-Fe_2O_3 (maghemite)	350, 500, 700
	α-Fe_2O_3 (hematite)	225, 247, 299, 412, 497, 613
Observed	Iron oxide	667
	OA-iron oxide	674, 1597

polymer was due to the fact that no specific binding sites had been created for the analyte. After leaching out uranium from the polymer matrix from the magnetic IIP, a relatively rough and irregular uneven morphology was observed. The formed cavities in the magnetic IIP were caused by the structure of the target uranium ion.

Table 2 Elemental analysis of OA coated magnetite

Mass (mg)	% C	% H	Ligand concentration (mmol g^{-1})[a]
2.05	4.63	1.38	3.86
2.01	4.82	1.46	3.99
2.01	4.48	1.39	3.71

[a] Values for the ligand concentration were all based on carbon content

The magnetic properties of the magnetic particles were recorded by vibrating sample magnetometry (VSM) at room temperature and the hysteresis curves, as a result of superparamagnetism, are shown in Fig. 4. The magnetism, based on saturation magnetism, decreased from bare Fe_3O_4, OA@Fe_3O_4 to magnetic IIP with saturation magnetizations (M_s) of 74.8, 3.7 and 1.6 emu g^{-1}, respectively. The magnetic IIP had the least magnetization because the magnetite was deeply embedded in the polymer matrix. The superparamagnetism of magnetic particles prevented them from aggregating even after the magnetic field was removed.

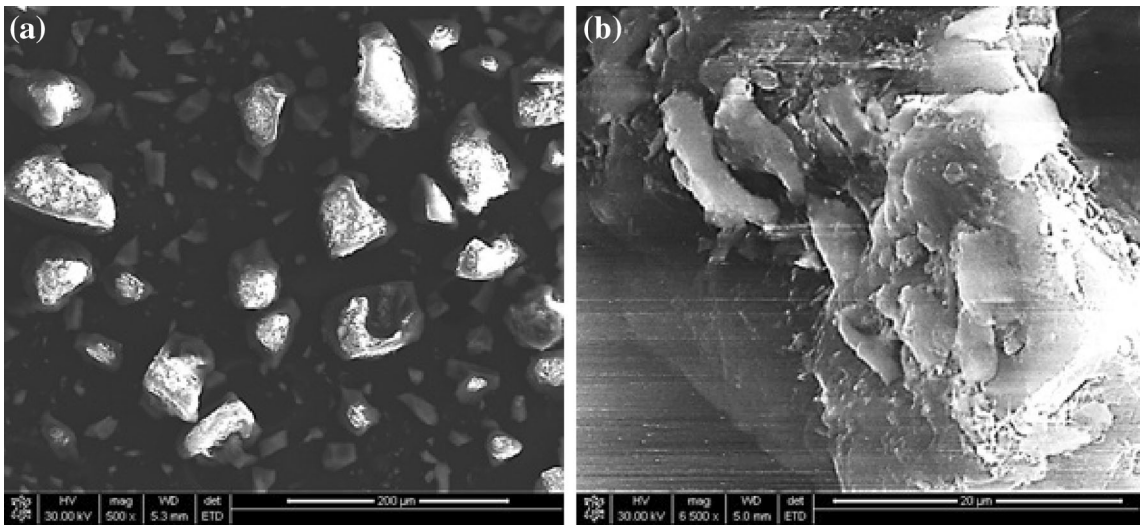

Fig. 3 SEM of magnetic **a** MIP and **b** NIP

Effect of sample pH and point of zero charge

Results of the influence of initial sample pH in uranyl(VI) adsorption on magnetic polymers was investigated (data not presented). There was a low uptake of the uranyl ions in acidic pH because of the competition of adsorption cavities by the smaller H^+ ions. However, as the pH increased, the competition became less and the uranyl ions outnumbered the protons, and there was a preferential sorption of the uranyl target. The maximum uptake of the uranyl was observed at pH 4 were there was an optimum uptake unto the magnetic polymers. This extraction efficiency was then maintained up to high basic pH values. Apart from the adsorption process from the bulk solution due to concentration gradient into fabricated adsorption sites, there was also a parallel formation of polymeric species such as $(UO_2)_2(OH_2)_2^{2+}$ and $(UO_2)_3(OH_2)_4^{2+}$ which precipitated out of solution. In another work, all the four magnetic nanoparticles coated with chitosan-epichlorohydrin beads prepared by Saifuddin and Dinara [22] showed optimum uranium extraction efficiency at pH 3 which was comparable with the value obtained in this work. According to Liu et al. [20], at pH <4.5, the =N– and –OH functionalities in quinoline-8-ol functional monomer were protonated leading to the reduction in the uptake of the uranyl ion by the polymer. This phenomenon was also likely to be present in our sorbent where the same functional groups were protonated and an electrostatic repulsion of the positively charged uranyl species with the magnetic sorbent was experienced.

The point of zero charge (pHpzc), a characteristic of any sorbent in surface science, was also determined to investigate the surface charge and acidic-basic character of the magnetic polymer (Fig. 5). The surface of this sorbent had hydroxyl and amine groups which are largely dependent on the pH of the solution. The graph of initial pH (pH_i) versus change in final pH (pH_f) was plotted and the pHpzc was determined to be a value where pH_f remains constant and was found to be 9.8. The surface charge of the magnetic polymer was positive at pH < 9.8 and negative at pH > 9.8. The surface charge of magnetic polymer is positive at pH < pHpzc, thus the decrease of UO_2^{2+} uptake on magnetic polymer at low pHs may be explained in terms of pHpzc. The electrostatic repulsion between UO_2^{2+} and positive surface of the magnetic polymer becomes stronger at pH < pHpzc.

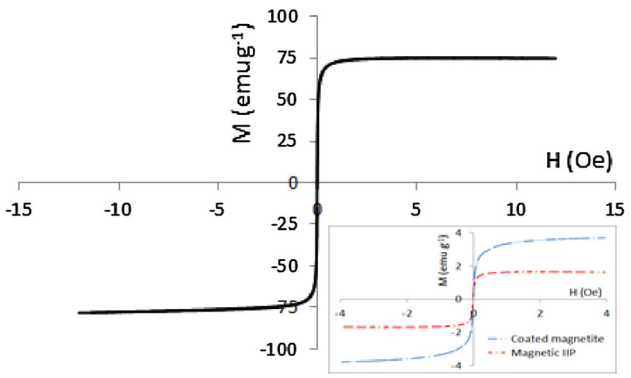

Fig. 4 Magnetization curves obtained by VSM for **a** Fe_3O_4, **b** OA@Fe_3O_4 and **c** magnetic IIP (all measured at room temperature)

Effect of amount of adsorbent

The effect of magnetic polymer amount on U(VI) adsorption by varying the amount from 10–100 mg of 2 mg L^{-1}

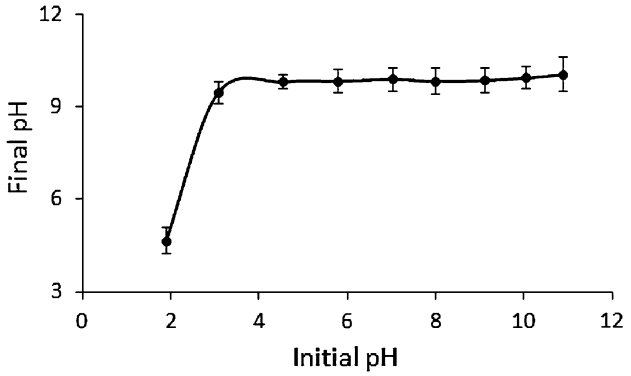

Fig. 5 pH_i versus pH_f for point of zero charge determination

U(VI) solution is shown in Table 3. The extraction efficiency was increased from 47 to 80 % and 35 to 62 % with an increase in amount of adsorbent from 10 to 50 mg for the magnetic IIP and NIP, respectively. The increase in the extraction efficiency with an increase in the magnetic polymer amount was probably due to the increase in surface area and adsorption sites available for adsorption [30]. A lower sorbent amount of 20 mg was found to be optimum by Pakade et al. [19] after they prepared a uranyl IIP through formation of a ternary complex of the target with 1-(prop-2-en-1-yl)-4–(pyridin-2-ylmethyl) piperazine and methacrylic acid.

Effect of contact time on the adsorption

The removal efficiency of U(VI) ions as a function of contact time is shown in Table 3. Batch adsorptions studies were carried out for contact times ranging from 10–90 min under experimental conditions outlined. Kinetics of adsorption of uranium(VI) consisted of two phases. The initial stages of the adsorption profile experienced a fast uranyl uptake where there is an instantaneous external surface adsorption. In this phase, U(VI) ions adsorption onto the magnetic polymers increased with an increase of contact time and reached adsorption equilibrium within 45 min. This fast adsorption equilibrium was probably due to high complexation and geometric shape affinity between U(VI) ions and its cavities in the magnetic polymeric matrix. In the second phase, there was a gradual adsorption and its contribution to the total U(VI) ions adsorption was relatively small where intra-particle diffusion controlled the adsorption rate. The faster adsorption rates with other adsorbents reported elsewhere could be attributed to the absence of internal diffusion resistance [18, 23]. The matrix of the polymer is embedded with magnetic cores which might limit the accessibility of internal pores by the uranyl ions, thereby making the adsorption kinetics faster than polymeric sorbents without solid cores endowed in their matrices.

Table 3 Effects of varying levels of different parameters on the uptake of U(VI) by magnetic polymers

No.	Parameter	Magnetic IIP	Magnetic NIP
1	Amount of magnetic polymer[a] (mg)	Extraction efficiency (%)	
	10	47.1 ± 5.3	34.5 ± 4.7
	25	76.3 ± 4.3	61.0 ± 5.5
	50	79.0 ± 1.2	62.4 ± 2.6
	75	82.3 ± 2.0	61.7 ± 3.0
	100	83.2 ± 1.5	61.0 ± 1.5
2	Agitation time[b] (min)	Adsorption capacity (mg g^{-1})	
	10	0.56 ± 0.02	0.45 ± 0.01
	20	0.65 ± 0.01	0.54 ± 0.02
	45	0.77 ± 0.02	0.67 ± 0.02
	60	0.85 ± 0.01	0.75 ± 0.01
	75	0.85 ± 0.01	0.77 ± 0.01
	90	0.85 ± 0.01	0.77 ± 0.01
3	Initial U(VI) concentration[c] (mg L^{-1})	Adsorption capacity (mg g^{-1})	
	0.5	0.2 ± 0.02	0.19 ± 0.02
	1.0	0.40 ± 0.02	0.36 ± 0.02
	1.5	0.61 ± 0.02	0.55 ± 0.02
	2.0	0.82 ± 0.02	0.74 ± 0.05
	2.5	1.03 ± 0.03	0.91 ± 0.01
	5.0	1.05 ± 0.03	0.95 ± 0.02
	8.0	1.01 ± 0.05	0.95 ± 0.03

[a] Adsorption conditions: Sample pH, 4; sample volume, 25 mL; uranium concentration, 2 mg L^{-1} contact time, 45 min; stirring speed, 1,500 rpm; temperature, 25 °C

[b] Adsorption conditions: Sample pH, 4; sample volume, 25 mL; uranium concentration, 2 mg L^{-1} polymer amount, 50 mg; stirring speed, 1,500 rpm; temperature, 25 °C

[c] Adsorption conditions: Sample pH, 4; sample volume, 25 mL; contact time, 45 min; polymer amount, 50 mg; stirring speed, 1,500 rpm; temperature, 25 °C

Effect of initial concentration

The initial concentration of U(VI) in the solution was varied between 0.5 and 8 mg L^{-1} for adsorption by maintaining the quantity of magnetic polymer dosage of 50 mg/25 mL as shown in Table 3. The increase in adsorption amount with increasing initial uranyl ion concentration from the bulk solution onto the magnetic adsorbent was probably due to the rise in the transfer force and the mass transfer level. This trend of adsorption continued until a saturation value was achieved at U(VI) ion concentration of 2 mg L^{-1}. Maximum adsorption capacities were 1.04 ± 0.03 and 0.95 ± 0.02 mg g^{-1} for the magnetic IIP and NIP, respectively. For Zhang et al. [21], the maximum uranyl retention capacities of IIP and CP polymer particles were 15.3 and 11.2 mg g^{-1}. These values are higher than what was obtained in our work. This might be probably due to the presence of shallow pores in our sorbent as a result of the incorporated magnetic cores.

Selectivity studies

The selectivity experiments of the magnetic polymers were conducted using Ni(II) and Th(IV) interferents as they widely co-exist with of U(VI) in water bodies. U(VI) was preferentially adsorbed due to the imprinting effect (Fig. 6). Table 4 summarizes the distribution ratios (K_d), selectivity coefficients (K) and relative selectivity coefficients (K') of the uranyl ions over Th(IV) and Ni(II) ions, calculated using Eqs. (3), (4) and (5), respectively. The distribution ratios of the Th(IV), Ni(II) and U(VI) were 979, 513 and 2789, respectively. Based on these values, the selectivity order of ions adsorbed onto magnetic polymers can be deduced as: U(VI) > Th(IV) > Ni(II). The K value of U(VI) binding in the presence of Th(IV) ions was found to be 2.8. For Ni(II), a K value of 5.4 obtained meant the sorbent extracted U(VI) 5.4 times more than it extracted Ni(II) ions, thereby making Ni(II) a less competitor than Th(IV). The non discriminate and lack of selectivity of the magnetic NIPs is evident from the The K values for the magnetic NIPs which were of the same order of magnitude of around 1.1 for both competitors. In magnetic IIPs, cavities are created after removal of the template which is complementary to the uranyl imprint ion in size and coordination geometry. However, there were no such cavities and recognition sites formed in the corresponding magnetic NIP and there were only non-specific interactions with the U(VI) ions and its competitors.

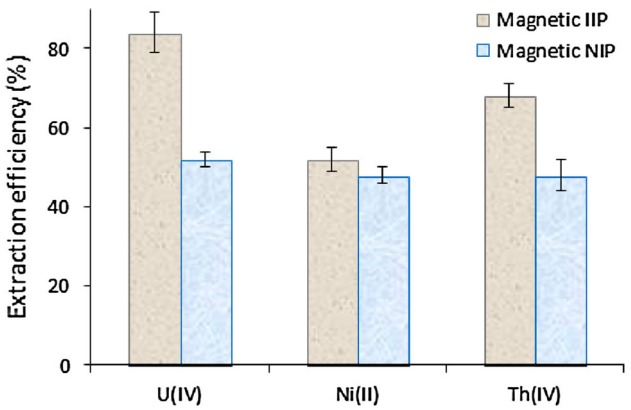

Fig. 6 Extraction efficiencies of the ions extracted by the magnetic IIP and NIP from the spiked 2 mg L^{-1} equimolar multi-elemental mixture of solutions (Amount of materials, 50 mg; solution pH 4; solution volume, 25 mL; contact time, 45 min)

Table 4 K_d, K and K' values for the magnetic IIP and NIP in multi-elemental mixture of solutions

	K_d (mL g^{-1})		K		K'
	IIP	NIP	IIP	NIP	
U(VI)	2,789	501	–	–	–
Ni(II)	513	426	5.4	1.2	4.6
Th(VI)	979	447	2.8	1.1	2.5

Regeneration and reusability

The regeneration of the sorbent is likely to be a key factor in improving process economics. To elute the accumulated uranyl ions from the magnetic sorbents and to regenerate them, 1 mol L^{-1} HCl was used. The re-usability of both the magnetic IIP and NIP was tested by running six adsorption–desorption cycles. The extraction efficiencies of magnetic IIP at beginning of the cycle and the last cycle had a small decrease of 3 % (Fig. 7). This implied that the prepared polymers can be reused.

Application of magnetic IIP to wastewater samples

In order to evaluate the applicability of the proposed method, it was applied to two real water samples, wastewater from treatment plant (WWTP) and acid mine drainage (AMD). All the solid particles were filtered of soon sampling in the laboratory. The unspiked water samples were then injected into ICP-OES to determine the uranium concentration. Spiked real water samples, adjusted to pH 4, were subjected to the magnetic IIPs for uranium extraction using the optimum conditions: Amount of materials, 50 mg; sample volume, 25 mL; contact time, 45 min. The un-extracted uranium content was then analysed for uranium and the results for the recoveries are shown in Table 5. The average extraction efficiencies of were determined to be 82 and 76 % for WWTP and AMD, respectively. This demonstrated the suitability of the

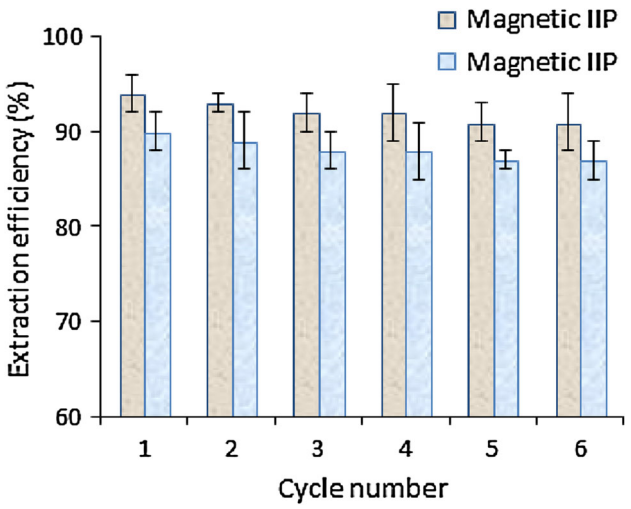

Fig. 7 Reusability and stability of magnetic polymers (Amount of materials, 50 mg; solution pH 4; solution volume, 25 mL; contact time, 45 min, U(VI) concentration, 2 mg L^{-1}, Desorption conditions: Solution volume, 25 mL; contact time, 45 min, [HCl] leachant, 1 mol L^{-1})

sorbent to selectively extract U(VI) ions from aqueous matrices.

Adsorption modelling

The Langmuir model provides some mechanistic understanding of the sorption phenomena but, and can conveniently be used to estimate the maximum uptake of uranium from the experimental data. This model is based on two main assumptions that the forces of interaction between adsorbed molecules are negligible and once an analyte occupies a site, no further sorption takes place (monolayer sorption). The linearized mathematical representation of its form can be expressed in the following form:

$$\frac{1}{q_e} = \frac{1}{q_m b C_e} + \frac{1}{q_m} \tag{6}$$

where C_e (mg L^{-1}) is the equilibrium concentration of U(VI) in the solution and q_e (mg g^{-1}) is the mass of U(VI) retained on a unit mass os the sorbent. q_m is the maximum adsorption capacity (mg g^{-1}) calculated from the slope and intercept of the straight-line plots of $1/q_e$ versus $1/C_e$ and b is the Langmuir constant.

According to the Langmuir model, the essential characteristics of the isotherm by means of a dimensionless constant separation factor (R_L) can be used to predict the favourability of interaction between the adsorbate and the adsorbent. This parameter is represented Eq. (7):

$$R_L = \frac{1}{(1 + bC_o)} \tag{7}$$

The Freundlich isotherm model predicts the adsorption intensity of the sorbent towards the adsorbent. It is often useful for modelling adsorption onto solids with heterogeneous surfaces [31]. It is an empirical equation employed to describe the isotherm data. It assumes multilayer adsorption and is applicable to adsorption of analytes onto heterogeneous adsorbent surface and can be expressed as Eq. (8):

$$lnq_e = lnK_f + \frac{1}{n} lnC_e \tag{8}$$

A plot of lnq_e versus lnC_e gives a linear graph where indicators of adsorption effectiveness, K_f and n, are calculated from the intercept and slope, respectively. The Freundlich coefficients (n) were found to be 1.07 and 1.11 for the magnetic IIP and NIP, respectively. According to Treyball [32], for the values of n between 1 and 10 the adsorbent is considered as good and this implies that the magnetic polymers synthesized were effective in the uptake of uranium.

The adsorption modelling parameters are summarized in Table 6 where the Langmuir is the best fitting model because it gives a higher correlation coefficient (>0.98). Satisfactory fitting of the Langmuir model to the adsorption isotherms of uranium sorption onto various polymeric sorbents adsorbents have also been reported [33–35]. Applicability of Langmuir model describes the monolayer adsorption of uranium on the homogeneous energetically equivalent surface of the magnetic polymer. It is derived from simple mass action kinetic, assuming chemisorption interactions. Chemisorption was likely to be from the acceptation of electrons by the positively charged uranyl ion from the N and O electron donors of the functional monomers.

Table 5 Application of magnetic polymers on wastewater samples

Wastewater	Concentration (mg g^{-1})		% Recovery
	Spiked	Found	
WWTP	–	DL$^{\neq}$	–
	1.00	0.83 (0.05)	83
	5.00	4.05 (0.02)	81
AMD	–	8.50 (0.02)	–
	5	12.10 (0.03)	76

DL$^{\neq}$: Below detection limit and SD values in parenthesis

Kinetics of adsorption

Two kinetic models, namely pseudo first-order and pseudo second-order models were employed to describe the adsorption process and the controlling adsorption mechanisms such as mass transfer and chemical reaction. The linear form of the pseudo first-order kinetic model is given by Eq. (9).

Table 6 The Langmuir and Freundlich constants for adsorption of U(VI) on magnetic polymers

Polymer	Langmuir constants				Freundlich constants		
	b (L g^{-1})	q_m (mg g^{-1})	R_L	R^2	n	K_f (L g^{-1})	R^2
Magnetic IIP	0.95	2.9	0.34	0.982	1.07	2.07	0.98
Magnetic NIP	0.66	2.6	0.43	0.992	1.11	1.24	0.99

Table 7 Calculated kinetic parameters of pseudo-first and second orders for initial U(VI) concentration of 2 mg L^{-1}

Polymer	Pseudo first-order			Pseudo second-order		
	R^2	k_1 (min^{-1})	q_e (mg g^{-1})	R^2	k_2 (g mg^{-1} min^{-1})	q_e (mg g^{-1})
Magnetic IIP	0.979	0.071	0.659	0.9982	0.163	0.923
Magnetic NIP	0.991	0.057	0.612	0.9977	0.163	0.864

$$log(q_e - q_t) = logq_e - \frac{k_1}{2.303}t \quad (9)$$

where q_e and q_t are the amounts of U(VI) adsorbed on adsorbent (mg g^{-1}) at equilibrium and at time t (min), respectively and k_1 (min^{-1}) is the rate constant of first-order adsorption. The rate constants, k_1 and q_e were deduced from the straight line plots of $log(q_e - q_t)$ versus t. The pseudo second-order equation is expressed as Eq. (10).

$$\frac{t}{q_t} = \frac{1}{k_2 q_e^2} + \frac{1}{q_e}t \quad (10)$$

where k_2 is the rate constant of second-order adsorption (g mg^{-1} min^{-1}). The values of the model parameters were calculated from the intercept and slope of the kinetic plots (graphs not presented). Based on calculated results shown in Table 7, the pseudo second order model is appropriate to predict the adsorption kinetics of U(VI) ions from aqueous solutions onto magnetic imprinted polymers. This model gave a good linear regression coefficient ($R^2 > 0.99$). Other researchers who used almost similar sorbents also obtained the pseudo second order as the best fitting model [21, 36, 37].

Comparative studies

A table, with a comparative assessment of U(VI) removal with various other sorbents reported in the literature was compiled (Table 8). In this work, the maximum adsorption capacity was found to be around 1.04 and 0.95 mg g^{-1} for

Table 8 Performance comparison of different U(VI) ion imprinted polymer sorbents (magnetic and non-magnetic)

Functional monomer	q (mg g^{-1})	t (min)	pH	Sorbent dosage (mg L^{-1})	Reference
Non-magnetic imprinted polymers					
1-(prop-2-en-1-yl)-4-(pyridin-2-ylmethyl)piperazine and methacrylic acid	120	20	4–8	667	Pakade et al. [19]
Salicylaldoxime and 4-vinylpyridine	151[a]	10	5	100	Singh and Mishra [25]
Aniline and 8-hydroxy quinoline functionalized aniline	22,410[a]	30	7	4	Milja et al. [39]
4-vinylpyridine	134	180	7	2,500	Anirudhan et al. [40]
5,7-dichloroquinoline-8-ol-4-vinylpyridine ternary	34	10	5–7	100	Gladis and Rao [41]
Magnetic imprinted polymers					
2,4-dioxopentan-3-yl methacrylate	15.3	720	–	20	Zhang et al. [21]
Salicylaldoxime and 4-vinylpyridine	1.2	45	4	2,000	Tavengwa et al. [30]
1-hydroxy-2-(prop-2′-enyl)-9,10-anthraquinone (HAQ)	14.1[a]	5	4–7	5,000	Fasihi et al. [33]
Chitosan	8.6	30	3.5	5,000	Wang et al. [42]
Activated carbon	28.5	240	5		Kütahyali and Eral [43]
Salicylaldoxime and 4-vinylpyridine	1.01	45	4	2,000	This work

[a] Converted from mmol g^{-1}; – Data not provided

the magnetic IIP and NIP, respectively. These values are observed to be low as we suspect the magnetic solid particles to be in the pores of the sorbent. As a consequence, this has an effect of lowering adsorption capacities (Table 8). The common non-magnetic polymers are included in the table to compare the sorption capacities which were generally higher than the magnetic particles embedded ones. However, there are other sorbents not embedded with solid cores which showed low sorption capacities than reported in this paper, with values as low as 0.0812 and 0.185 mg g^{-1} for two sorbents, even after functionalization [38].

Conclusions

In the present work, a ternary complex of UO_2^{2+} with SALO, 4-VP and MAA was synthesized and was made magnetic by embedding OA coated magnetic nano-particles into polymeric matrix of IIPs and NIPs during the cross-linking stage. The sorbent was then successfully used for the removal of uranyl ions from aqueous solutions and various parameters that gave the optimum uptake of the uranyl ions were determined. Due to the selectivity shown by these composite polymers for uranyl ions, the material can be applied for selective separation and pre-concentration of uranyl ions from aqueous samples.

Acknowledgments The authors would like to thank the Water Research Commission (WRC) of South Africa (Project Number 2014) and the University of Witwatersrand for providing financial support through the Wits Postgraduate Merit Award.

References

1. Al-Sheikhly M, Barkatt A, Laverene J (2012) Enhancement of the extraction of the uranium from seawater. US Department of Energy, p 1
2. Kavakli P, Guven J (2004) Removal of concentrated heavy metal ions from aqueous solutions using polymers with enriched amidoxime groups. J Appl Polym Sci 93:1705–1710
3. Vogel C, Exner RM, Adam C (2013) Heavy metal removal from sewage sludge ash by thermochemical treatment with polyvinylchloride. Environ Sci Technol 47:563–567
4. Aksu Z (2005) Application of biosorption for the removal of organic pollutants: a review. Process Biochem 40:997–1026
5. Singh U, Kaushal RK (2013) Treatment of wastewater with low cost adsorbent: a review. VSRDIJTNTR 4:33–42
6. Surchi KMS (2011) Agricultural wastes as low cost adsorbents for Pb removal: kinetics, equilibrium and thermodynamics. IJC 3:103–112
7. Jirekar D, Dar BA, Farooque M (2013) Husk of gram seeds as a low-cost adsorbent for the removal of methylene blue dye from aqueous solutions. JESWR 2:226–232
8. Singh K, Shah C, Dwivedi C, Kumar M, Bajaj PN (2013) Study of uranium adsorption using amidoximated polyacrylonitrile-encapsulated macroporous beads. J Appl Polym Sci 127:410–419
9. Sugo T (1997) Status of development for recovery technology of uranium from seawater. Nippon Kaisui Gakkai-Shi 51:20–27
10. Kubota H, Shigehisa Y (1995) Introduction of amidoxime groups into cellulose and its ability to adsorb metal ions. J Appl Polym Sci 56:147–151
11. Contreras-Garcia A, Burillo G, Aliev R, Bucio E (2008) Radiation grafting of N, N′-dimethylacrylamide and N-isopropylacrylamide onto polypropylene films by two-step method. Radiat Phys Chem 77:936–940
12. Saad DMG, Cukrowska ME, Tutu H (2013) Modified cross-linked polyethylenimine for the removal of selenite from mining wastewaters. Toxicol Environ Chem 95:409–421
13. Murray GM, Uy OM (2001) In: Sellergren B (ed) Molecularly imprinted polymers. Elsevier, The Netherlands, p 441
14. Haupt K, Mosbach K (2000) Molecularly imprinted polymers and their use in biomimetic sensors. Chem Rev 100:2495–2504
15. Mosbach K, Ramstrom O (1996) The emerging technique of molecular imprinting and its future impact on biotechnology. Nat Biotechnol 14:163–170
16. Shea KJ (1994) Molecular imprinting of synthetic network polymers: the de novo synthesis of macromolecular binding and catalytic sites. Trends Polym Sci 2:166–173
17. Baes CFJ, Mesmer RE (1976) The hydrolysis of cations. Wiley, New York
18. Liu Y, Cao X, Hua R, Wang Y, Liu Y, Pang C, Wang Y (2010) Selective adsorption of uranyl ion on ion-imprinted chitosan/PVA cross-linked hydrogel. Hydrometallurgy 104:150–155
19. Pakade VE, Cukrowska EM, Darkwa J, Darko G, Torto N, Chimuka L (2012) Simple and efficient ion imprinted polymer for recovery of uranium from environmental samples. Water Sci Technol 65:728–736
20. Liu Y, Cao X, Le Z, Luo M, Xu W, Huang G (2010) Pre-concentration and determination of trace uranium(VI) in environments using ion-imprinted chitosan resin via solid phase extraction. J Braz Chem Soc 21:533–540
21. Zhang H, Liang H, Chen Q, Shen X (2013) Synthesis of a new ionic imprinted polymer for the extraction of uranium from seawater. J Radioanal Nucl Chem 298:1705–1712
22. Saifuddin N, Dinara S (2012) Immobilization of *Saccharomyces cerevisiae* onto cross-linked chitosan coated with magnetic nanoparticles for adsorption of uranium(VI) ions. Adv Nat Appl Sci 6:249–267
23. Sadeghi S, Aboobakri E (2012) Magnetic nanoparticles with an imprinted polymer coating for the selective extraction of uranyl ions. Microchim Acta 178:89–97
24. Tavengwa NT, Cukrowska E, Chimuka L (2014) Preparation, characterization and application of $NaHCO_3$ leached bulk U(VI) imprinted polymers endowed with γ-MPS coated magnetite in contaminated water. J Hazard Mater 267:221–228
25. Singh DK, Mishra S (2009) Synthesis and characterization of UO_2^{2+}-ion imprinted polymer for selective extraction of UO_2^{2+}. Anal Chim Acta 644:42–47
26. Kumar PS, Kirthika K (2009) Equilibrium and kinetic study of adsorption of nickel from aqueous solution onto bael tree leaf powder. JESTEC 4:351–363
27. Zeinali F, Ghoreyshi AA, Najafpour GD (2010) Adsorption of dichloromethane from aqueous phase using granular activated carbon: isotherm and breakthrough curve measurement. Middle-East J Sci Res 5:191–198
28. Slavov L, Abrashev MV, Merodiiska T, Gelev C, Vandenberghe RE, Markova-Deneva I, Nedkov I (2010) Raman spectroscopy investigation of magnetite nanoparticles in ferrofluids. J Magn Magn Mat 322:1904–1911
29. Tang J, Myers M, Bosnick KA, Brus LE (2003) Magnetite Fe_3O_4 nanocrystals: spectroscopic observation of aqueous oxidation kinetics. J Phys Chem B 107:7501–7506

30. Tavengwa NT, Cukrowska E, Chimuka L (2014) Synthesis of bulk ion-imprinted polymers (IIPs) embedded with oleic acid coated Fe_3O_4 for selective extraction of hexavalent uranium. Water SA 4:623–630
31. Stumn W, Morgan JJ (1981) Aquatic chemistry. Wiley, New York
32. Treyball RE (1980) Mass transfer operations, 3rd edn. McGraw Hill, New York
33. Fasihi J, Alahyari SA, Shamsipur M, Sharghi H, Charkhi A (2001) Adsorption of uranyl ion onto an anthraquinone based ion-imprinted copolymer. React Funct Polym 71:803–808
34. Ilaiyaraja P, Deb AKS, Sivasubramanian K, Ponraju D, Venkatraman B (2013) Adsorption of uranium from aqueous solution by PAMAM dendron functionalized styrene divinylbenzene. J Hazard Mater 250–251:155–166
35. Tripathi A, Melo JS, D'Souza SF (2013) Uranium(VI) recovery from aqueous medium using novel floating macroporous alginate-agarose-magnetite cryobeads. J Hazard Mater 246–247:87–95
36. Anirudhan TS, Divya L, Suchithra PS (2009) Removal and recovery of uranium(VI) by adsorption onto a lignocellulosic-based polymeric adsorbent containing amidoxime chelating functional group. Toxicol Environ Chem 91:1237–1252
37. Heshmati H, Torab-Mostaedi M, Gilani HG, Heydari A (2014) Kinetic, isotherm, and thermodynamic investigations of uranium(VI) adsorption on synthesized ion-exchange chelating resin and prediction with an artificial neural network. Desalin Water Treat 35:1–12
38. Ting CF, Jie X, Wei Gu, Mei HJ, Sheng H, Lin WX (2013) Improvement in uranium adsorption properties of amidoxime-based adsorbent through cografting of amine group. J Dispers Sci Technol 34:604–610
39. Milja TE, Krupa VS, Rao TP (2014) Synthesis, characterization and application of uranyl ion imprinted polymers of aniline and 8-hydroxy quinoline functionalized aniline. RSC Adv 4:30718
40. Anirudhan TS, Nima J, Divya PL (2014) Adsorption and separation behavior of uranium(VI) by 4-vinylpyridine-grafted-vinyltriethoxysilane-cellulose ion imprinted polymer, J Environ Chem Eng. doi: 10.1016/j.jece.2014.10.006
41. Gladis JM, Rao TP (2004) Effect of porogen type on the synthesis of uranium ion imprinted polymer materials for the pre-concentration/separation of traces of uranium. Microchim Acta 146:251–258
42. Wang J, Peng R, Yang J, He Q and Liu Y (2011) Selective adsorp-tion of uranium(VI) on U(VI) ion-imprinted chitosan composite magnetic microspheres. In: Proceedings of the Computer Distributed Control and Intelligent Environmental Monitoring (CDCIEM), Changsha, 19–20 Feb 2011, pp 1714–1717
43. Kütahyali C, Eral M (2004) Selective adsorption of uranium from aqueous solutions using activated carbon prepared from charcoal by chemical activation. Sep Purif Technol 40:109–114